ELECTRONIC SUPPLEMENTARY INFORMATION

H_2 activation by zirconaziridinium ions: σ-bond metathesis *versus* frustrated Lewis pairs reactivity

Peter H. M. Budzelaar,[*,a] *David L. Hughes,*[b] *Manfred Bochmann,*[b] *Alceo Macchioni*[c] *and Luca Rocchigiani*[*,b]

a. Department of Chemistry, University of Naples Federico II, Via Cintia, I-80126, Naples, Italy
email: p.budzelaar@unina.it
b. School of Chemistry, University of East Anglia, Norwich Research Park, NR4 7TJ, Norwich, UK
email: L.Rocchigiani@uea.ac.uk
c. Department of Chemistry, Biology and Biotechnology and CIRCC, University of Perugia, Via Elce di Sotto, 8, 06123, Perugia, Italy

CONTENTS:

1. Materials and methods

All manipulations of air-sensitive materials were performed in flamed Schlenk glassware or in a nitrogen-filled MBraun Unilab glovebox with high-capacity recirculatory (<1 ppm O_2 and H_2O). Deuterated solvents were freeze-pump-thaw degassed, distilled over CaH_2 and stored over activated 4Å molecular sieves in the glovebox. Cp_2ZrMe_2 and $[CPh_3][B(C_6F_5)_4]$ were synthesized according to literature procedures.[1] $[HNMe_2Ph][B(C_6F_5)_4]$ was purchased from Strem and used as received. Cp_2ZrH_2 was purchased from Sigma Aldrich and used as received.

Zirconaziridium ion pairs **1a** and **1b** were prepared as described previously.[2]

1a: 15 mg of Cp_2ZrMe_2 and 0.95 equivalent of $[CPh_3][B(C_6F_5)_4]$ (52.2 mg) were dissolved in C_6D_5Cl to give a bright red solution. Soon after, 1.05 equivalents of methyl-dihexylamine (16.0 μl) were added by using a microsyringe causing the solution to turn to yellow. Slow CH_4 evolution was observed over the period of 4h. Successively, the solution was dried under vacuum and the residual oily phase was rinsed with benzene (3x0.5 ml) and dried again. Solutions for hydrogenolysis were prepared by redissolving the oil in C_6D_5Cl.

1b: 15 mg of Cp_2ZrMe_2 and 1 equivalent of $[HNMe_2Ph][B(C_6F_5)_4]$ (47.8 mg) were loaded into a J-Young NMR tube and suspended in 0.6 ml of C_6D_6. Soon after mixing, an orange oily phase settled at the bottom of the NMR tube and a CH_4 evolution was observed. After 6 hours, the supernatant solution was removed, the oil was washed with benzene and the residues were dried under vacuum. Solutions for hydrogenolysis were prepared by redissolving the oil in C_6D_5Cl.

Experiments with H_2 were performed in J-Young NMR tubes on a dedicated Schlenk line interfaced with a Parker Domnic Hunter hydrogen generator (H_2 purity >99.9995%) at 1 atmosphere. In the typical procedure, NMR solutions were initially freeze-pump-thaw degassed three times to evacuate N_2. Successively, H_2 was introduced in the NMR tube and the solution was left equilibrating at the desired temperature.

^1H, ^1H inversion recovery, ^{19}F, $^{13}C\{^1H\}$, ^1H NOESY, ^{19}F,^1H HOESY, ^1H,^{13}C HMQC, and ^1H,^{13}C HMBC NMR experiments have been recorded on a Bruker DPX–300 spectrometer equipped with a ^1H,BB smartprobe and Z-gradients or on a Bruker Avance III HD 400 equipped with a ^1H,BB smartprobe and Z-gradients. ^1H NMR spectra are referenced to the residual protons of the deuterated solvent. ^{13}C NMR spectra are referenced to the D-coupled ^{13}C signals of the solvent. ^{19}F NMR spectra are referenced to an external standard of $CFCl_3$.

References

1) (a) E. Samuel and M. D. Rausch, *J. Am. Chem. Soc.*, 1973, **95**, 6263; (b) A.G. Massey and A.J. Park, *J. Organomet. Chem.*, 1964, **2**, 245.

2) L. Rocchigiani, G. Bellachioma, G. Ciancaleoni, A. Macchioni, D. Zuccaccia and C. Zuccaccia, *Organometallics*, 2011, **30**, 100.

2. Relevant NMR experiments and spectra

$[Cp_2ZrCH_2N(C_6H_{13})_2][B(C_6F_5)_4]$(1a) + H_2

A solution of **1a** in C_6D_5Cl was prepared in a J-Young NMR tube as reported before starting from 15 mg of Cp_2ZrMe_2. After degassing by freeze-pump-thaw, the solution was frozen and exposed to H_2 for 3 minutes. Successively, the tube was sealed and left to equilibrate at room temperature. After vigorous shaking to maximise H_2 solubilisation, the tube was inserted into the NMR probe and analysed at room temperature. Over the course of the experiment, a yellow oily phase settled at the bottom of the NMR tube. Conversion of **1a** into **2** + some minor impurities was observed over the period of 5 minutes.

^{1}H NMR (300.13 MHz, C_6D_5Cl, 297K, J values in Hz): 7.48 (s, 0.3, N-H), 6.03 (s, 5.7H, Cp of **2**), 2.35 (m, 4H, N-CH_2), 2.15 (s, 3H, N-Me), 1.36-1.09 (m, 18H, hexyl), 0.85 (br t, 8H, hexyl-Me), -3.87 (d, $^2J_{HH}$=11.9, 0.6H, Zr(μ^2-H) of **2**), -5.74 ppm (q, $^2J_{HH}$=11.9, 0.6H, Zr(μ^3-H) of **2**).

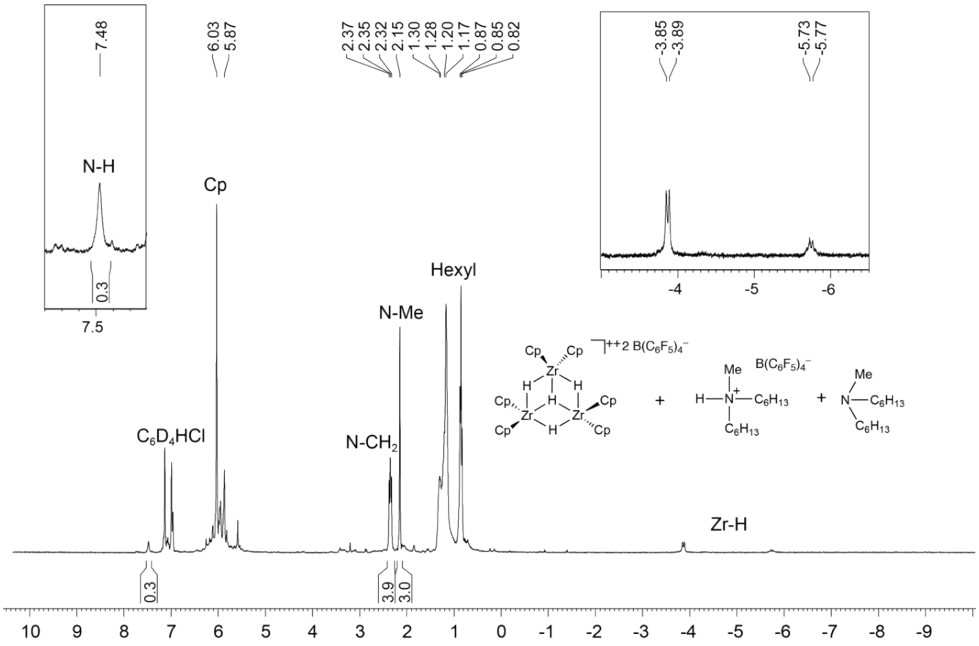

Figure S1. ^{1}H NMR spectrum obtained after reacting **1a** with H_2 for 5 minutes (C_6D_5Cl, 297K). Relative integration shows the presence of both $[HNMe(C_6H_{13})_2][B(C_6F_5)_4]$ and $NMe(C_6H_{13})_2$ in 1:2 ratio.

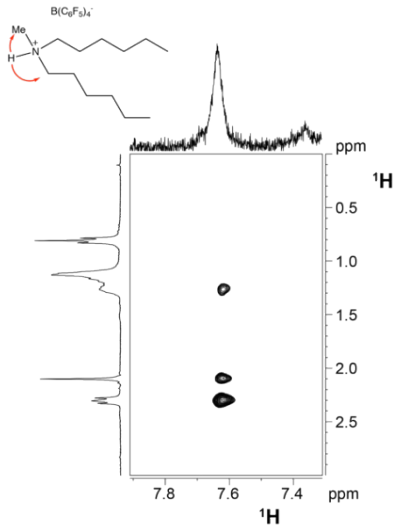

Figure S2. A section of the ^{1}H NOESY NMR spectrum obtained after reacting **1a** with H_2 for 5 minutes (C_6D_5Cl, 297K).

$[Cp_2ZrCH_2NMePh][B(C_6F_5)_4]$(1b) + H_2 at 297K

A solution of **1b** in C_6D_5Cl was prepared in a J-Young NMR tube as reported before starting from 15 mg of Cp_2ZrMe_2. After degassing by freeze-pump-thaw, the solution was frozen and exposed to H_2 for 3 minutes. Successively, the tube was sealed and left to equilibrate at room temperature. After vigorous shaking to maximise H_2 solubilisation, the tube was inserted into the NMR probe and analysed at room temperature. Over the course of the experiment, a yellow oily phase settled at the bottom of the NMR tube. Conversion of **1b** into **2** was complete in 24 hours.

^{1}H NMR (300.13 MHz, C_6D_5Cl, 297K, J values in Hz): 7.10 (m, overlapped with solvent, *m*-Ph), 6.93 (m, overlapped with solvent, *p*-Ph), 6.55 (d, $^3J_{HH}$=8.0, 2H, *o*-Ph), 6.42 (s, 0.5H, N-H), 6.00 (s, 6.2H, Cp of **2**), 2.47 (s, 6H, NMe_2), -3.87 (d, $^2J_{HH}$=11.9, 0.6H, Zr(μ^2-H) of **2**), -5.76 ppm (q, $^2J_{HH}$=11.9, 0.6H, Zr(μ^3-H) of **2**).

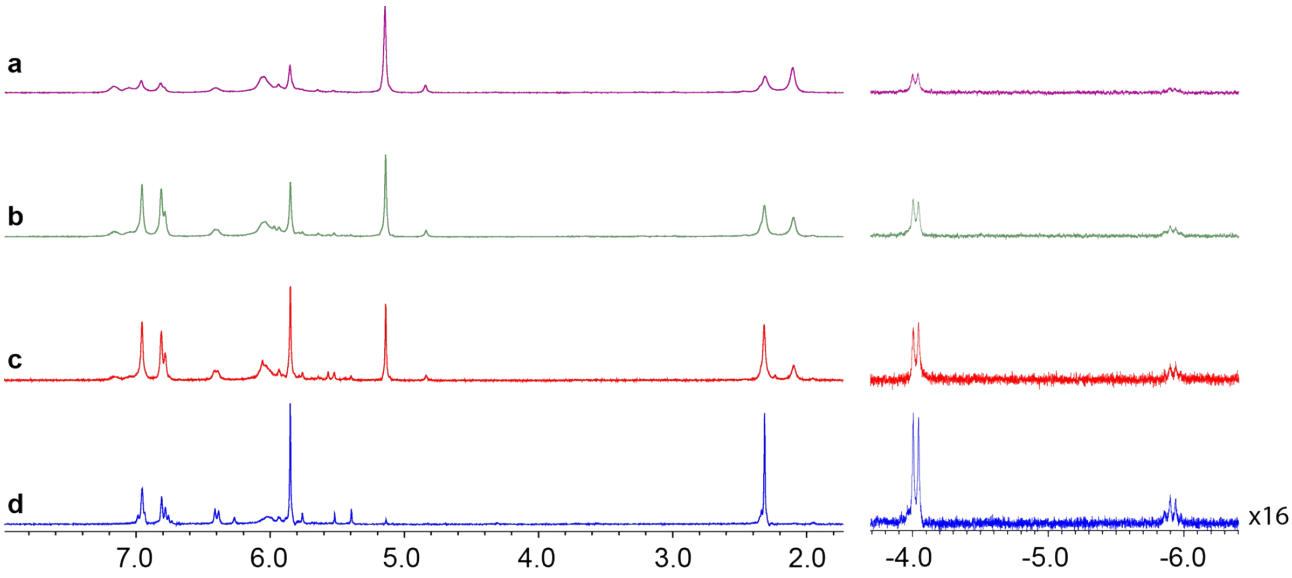

Figure S3. Evolution of the ^{1}H NMR spectrum of **1b** upon reacting with H_2 (297 K, C_6D_5Cl). Spectra recorded after 10 minutes (a), 30 minutes (b) 2 hours (c) and 24 hours (d) from the addition.

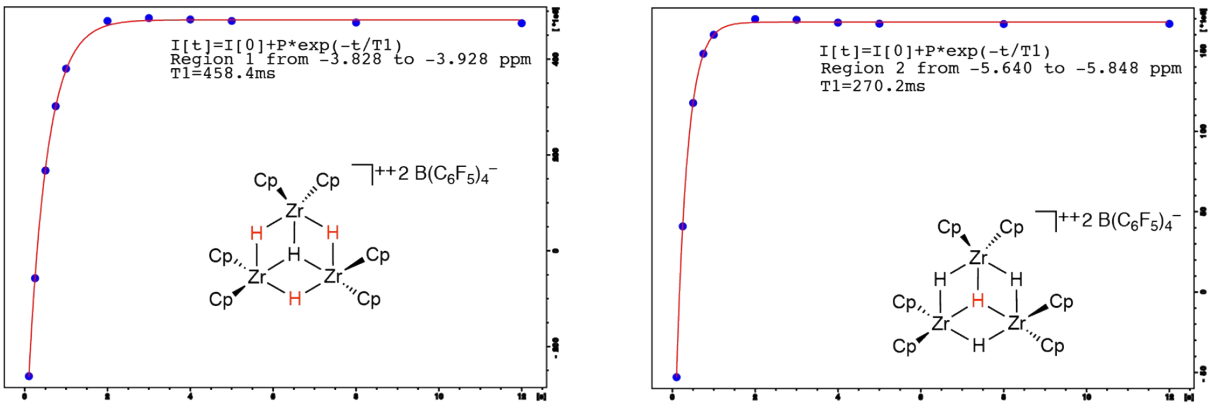

Figure S4. Inversion recovery profiles obtained for the bridging hydrides in **2** (C_6D_5Cl, 297K).

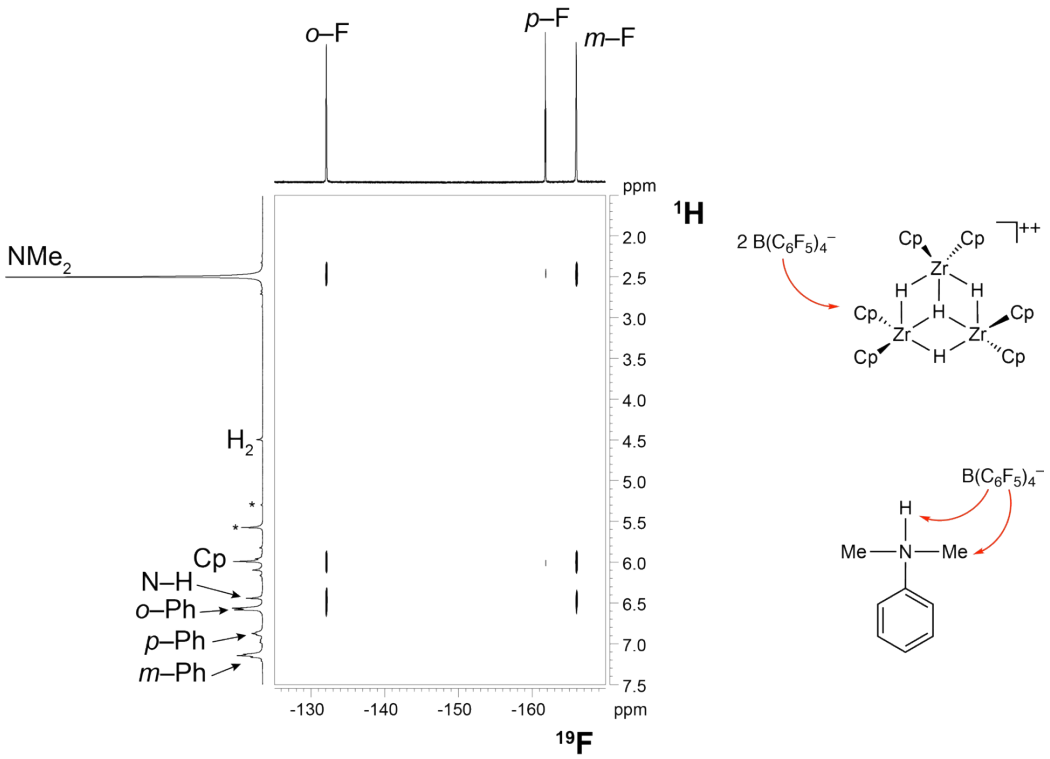

Figure S5. $^{19}F,^{1}H$ HOESY NMR spectrum acquired during the conversion of **1b** into **2** in C_6D_5Cl at 25°C; asterisk denote traces of **I**. NOE contacts for **I** were not detected under these conditions.

[Cp_2ZrCH_2NMePh][$B(C_6F_5)_4$](1b) + H_2 at 243K

A solution of **1b** in C_6D_5Cl was prepared in a J-Young NMR tube as reported before starting from 15 mg of Cp_2ZrMe_2. After degassing by freeze-pump-thaw, the solution was frozen and exposed to H_2 for 3 minutes. Successively, the tube was sealed and left to equilibrate with in a cold bath at ~ 243 K. After vigorous quick shaking to maximise H_2 solubilisation, the tube was inserted into the NMR probe and analysed at 243K. Full conversion of **1b** into **I** was achieved over 4 hours, by occasionally shaking the cold NMR tube.

^{1}H NMR (300.13 MHz, C_6D_5Cl, 243K, J values in Hz): 7.27 (t, $^{3}J_{HH}$=7.8, 2H, *m*-Ph), 7.14 (t, $^{3}J_{HH}$=7.4, 1H, *p*-Ph), 6.14 (d, $^{3}J_{HH}$=7.8, 2H, *o*-Ph), 5.19 (s, 10H, Cp), 4.72 (s, 1H, Zr-H), 2.18 ppm (s, 6H, NMe_2). $^{13}C\{^{1}H\}$ NMR (75.47 MHz, C_6D_5Cl, 243K, J values in Hz): 148.5 (br d, $^{1}J_{CF}$ = 240.0, $B(C_6F_5)_4^-$), 139.0 (s, C_{ipso}), 138.4 (br d, $^{1}J_{CF}$ = 245.0, $B(C_6F_5)_4^-$), 136.6 (br d, $^{1}J_{CF}$ = 245.0, $B(C_6F_5)_4^-$), 136.2 (s, *m*-Ph), 129.6 (s, buried under C_6D_5Cl, *p*-Ph), 108.7 (s, *o*-Ph), 107.7 (s, Cp), 50.8 ppm (s, NMe_2).

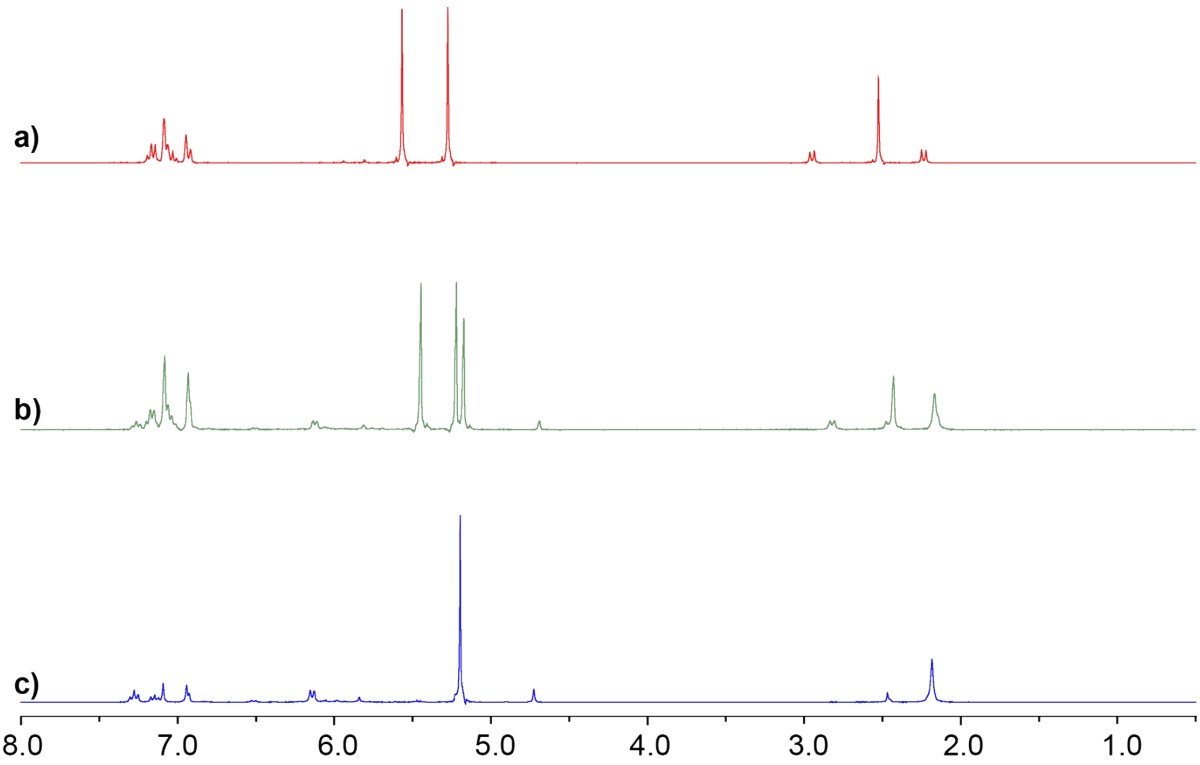

Figure S6. ^{1}H NMR spectra in C_6D_5Cl of: **1b** at 297 K (a); **1b** + H_2 after 1 hour at 243 K (b); **1b** +H_2 after complete conversion at 243K.

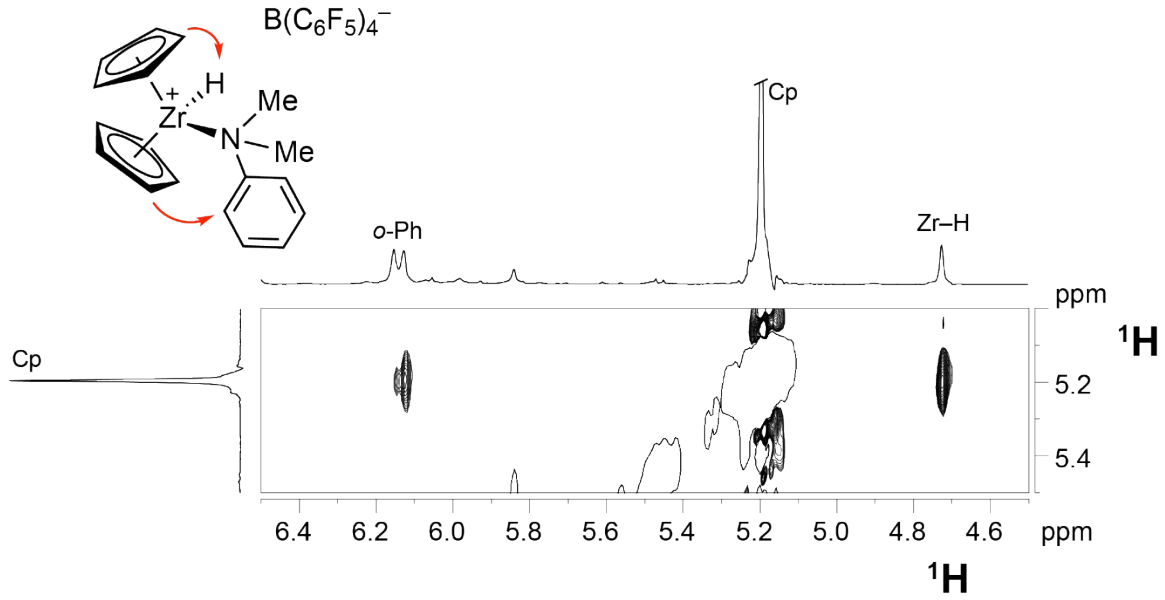

Figure S7. A section of the ^{1}H NOESY NMR spectrum of intermediate **I** at 243 K in C_6D_5Cl.

Cp_2ZrH_2+[$HNMe_2Ph$][$B(C_6F_5)_4$]

In the glovebox, 10 mg of Cp_2ZrH_2 and 0.67 equiv. of [$HNMe_2Ph$][$B(C_6F_5)_4$] were loaded into a J-Young NMR tube and suspended in 0.7 ml of C_6D_5Cl. Upon solvent addition, extensive gas evolution was observed, together with the precipitation of a yellow oily phase. After 10 minutes, the supernatant was removed, the oily phase was dried under vacuum and redissolved in dry CD_2Cl_2 to give a yellow solution, which showed the presence of **2** in 97% purity. **2** is not stable in dichloromethane and after a few hours, decomposition to unidentified species occurred.

^{1}H NMR (300.13 MHz, CD_2Cl_2, 297K, J values in Hz): 6.54 (s, 10H, Cp), -3.42 (d, $^2J_{HH}$=12, 3H, Zr(μ^2-H)), -5.29 ppm (q, $^2J_{HH}$=12.0, 1H, Zr(μ^3-H)). ^{13}C{^{1}H} NMR (75.47 MHz, C_6D_5Cl, 297K): 111.8 ppm (s, Cp).

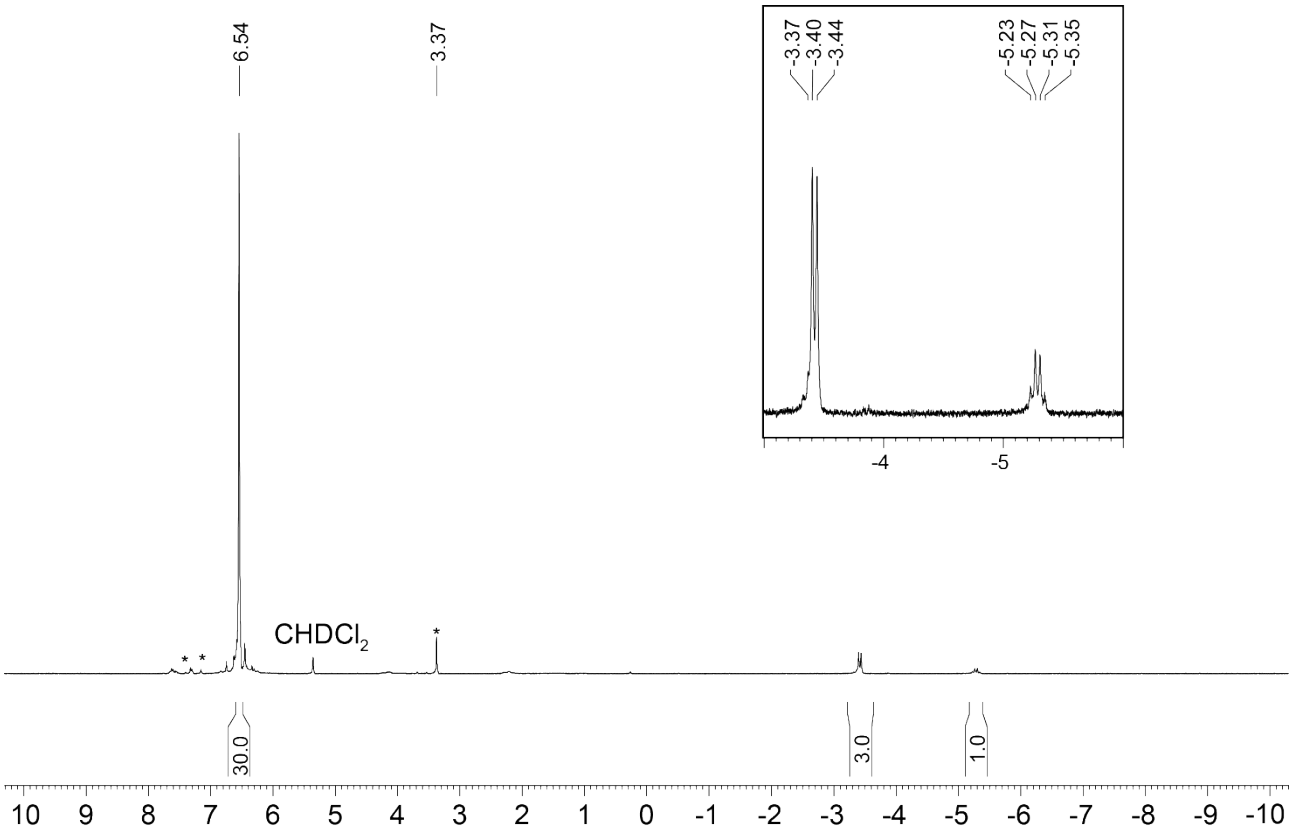

Figure S8. ^{1}H NMR spectrum of **2** (297 K, CD_2Cl_2) obtained after the reaction of Cp_2ZrH_2 with [$HNMe_2Ph$][$B(C_6F_5)_4$] in a 3:2 stoichiometric ratio; asterisk denote traces of anilinium salts.

3. X Ray diffraction

Crystal structure analysis of $H(Cp_2ZrH)_3$, $2(B(C_6F_5)_4)$, $5(C_6H_5Cl)$

Crystal data: $C_{30}H_{34}Zr_3$, $2(C_{24}BF_{20})$, $5(C_6H_5Cl)$, M = 2589.08. Orthorhombic, space group $Pna2_1$ (no. 33), a = 20.8992(3), b = 15.4821(2), c = 30.6370(4) Å, V = 9913.0(2) Å^3. Z = 4, Dc = 1.735 g cm^{-3}, F(000) = 5128, T = 100(2) K, μ(Mo-Kα) = 5.71 cm^{-1}, λ(Mo-Kα) = 0.71073 Å.

CCDC: 1970058

Crystals are colourless plates. From a sample under oil, one, *ca* 0.005 x 0.09 x 0.12 mm, was mounted on a Micro-mount/mesh and fixed in the cold nitrogen stream on a Rigaku OD XtaLAB AFC12 diffractometer (at the National Crystallographic Service in Southampton), equipped with a CCD plate detector, rotating anode generator with Mo-Kα radiation and a mirror monochromator. Intensity data were measured by thin-slice ω-scans. Total no. of reflections recorded, to θ_{max} = 27.5°, was 111217 of which 22692 were unique (Rint = 0.0035); 20023 were 'observed' with $I > 2\sigma_I$.

Data were processed using the CrysAlisPro[1] program. The structure was determined by the intrinsic phasing routines in the SHELXT program[2] and refined by full-matrix least-squares methods, on F^2's, in SHELXL[2]. The principal ions (cation and two anions) were fully resolved and the non-hydrogen atoms were refined with anisotropic thermal parameters. Hydrogen atoms in the cyclopentadienyl ligands were included in idealised positions and their Uiso values were set to ride on the Ueq values of the parent carbon atoms. There are five separate, unique solvent molecules in the asymmetric unit, most of them showing disorder; in all but one unit (comprising the overlaid molecules of Cl3, Cl7 and Cl8), the Cl and C atoms were refined anisotropically and hydrogen atoms were included as in the cation. The disorder in the Cl(3)/Cl(7)/Cl(8) unit is not fully resolved and no hydrogen atoms were included here. At the conclusion of the refinement, wR_2 = 0.113 and R_1 = 0.059 (2B) for all 22692 reflections weighted $w = [\sigma^2(F_o^2) + (0.0444P)^2 + 21.29P]^{-1}$ with $P = (F_o^2 + 2F_c^2)/3$; for the 'observed' data only, R_1 = 0.049.
In the final difference map, the highest peaks (*ca* 0.86 eÅ^{-3}) were near the zirconium atoms.

Scattering factors for neutral atoms were taken from ref. 3. Computer programs used in this analysis have been noted above, and were run through WinGX[4] at the University of East Anglia.

References

1 Program CrysAlisPro 1.171.40.45a, Rigaku OD (2019).
2 G. M. Sheldrick, SHELX – Programs for crystal structure determination (SHELXT) and refinement (SHELXL-2014), *Acta Cryst.* (2008) A**64**, 112-122, (2015) A**71**, 3-8 and (2015) C**71**, 3-8.
3 *'International Tables for X-ray Crystallography'*, Kluwer Academic Publishers, Dordrecht (1992). Vol. C, pp. 500, 219 and 193.
4 L. J. Farrugia, (2012) *J. Appl. Cryst.* **45**, 849–854.

Notes on the structure

The $H(Cp_2ZrH)_3$ cation is well-resolved, with the hydrogen atoms of the Zr_3H_4 core located and included in the refinement (with some constraints on their thermal parameters); these four H atoms refined more satisfactorily with site occupancies of 2.0. The two $B(C_6F_5)_4$ anions were also clear and all their atoms were refined anisotropically; there is motion in some of the C_6F_5 groups, but no indication of disorder.

The five solvent molecules, C_6H_5Cl, provided the challenges here – each is quite discrete and different. The molecule of Cl(2) is good except that some of the C atoms have large thermal ellipsoids; there is a minor, second Cl site, close to Cl(2), but the carbon atoms of the corresponding phenyl ring were not identified. The molecule of Cl(4) is fine and shows no disorder. In the molecule of Cl(5), there is a second chlorine atom, in the *para* position, whose phenyl carbon atoms are not distinct from those of the principal molecule although their thermal ellipsoids are all elongated parallel to the Cl(5)…Cl(54) vector. The molecule of Cl(6) is similar to that of Cl(2), with a minor chlorine atom in the *ortho* position and the carbon atoms of the alternative orientation not distinguished.

The molecule of Cl(3) is overlaid by the molecules of Cl(7) and Cl(8) facing in the opposite direction; the three molecules are essentially coplanar. The phenyl ring of C(131-136) is clear, but the rings of C(171-176) and C(181-186) are closely overlapping and not fully resolved. The Cl atoms Cl(3) and Cl(8) share the sites of the *para*-carbon atoms C(184) and C(134) of pseudo-symmetrically related molecules. The molecule of Cl(7) is rotated *ca* 30° from that of Cl(8), and these two molecules share (approximately) the sites of C(171/181), C(172/182) and C(176/186).

Crystal data and structure refinement for $H(Cp_2\ Zr\ H)_3$, $2(B(C_6F_5)_4)$, $5(C_6H_5Cl)$

Identification code	s0204
Elemental formula	C30 H34 Zr3, 2(C24 B F20}, 5(C6 H5 Cl)
Formula weight	2589.08
Crystal system, space group	Orthorhombic, $Pna2_1$ (no. 33)
Unit cell dimensions	a = 20.8992(3) Å α = 90 ° b = 15.4821(2) Å β = 90 ° c = 30.6370(4) Å γ = 90 °
Volume	9913.0(2) $Å^3$
Z, Calculated density	4, 1.735 Mg/m^3
F(000)	5128
Absorption coefficient	0.571 mm^{-1}
Temperature	100(2) K
Wavelength	0.71073 Å
Crystal colour, shape	colourless plate
Crystal size	0.12 x 0.09 x 0.005 mm
Crystal mounting:	on a glass fibre, in oil, fixed in cold N_2 stream
On the diffractometer:	
Theta range for data collection	2.352 to 27.485 °
Limiting indices	-27<=h<=26, -19<=k<=20, -39<=l<=39
Completeness to theta = 25.242	99.9 %
Absorption correction	Semi-empirical from equivalents
Max. and min. transmission	1.00000 and 0.83563
Reflections collected (not including absences)	111217
No. of unique reflections	22692 [R(int) for equivalents = 0.035]
No. of 'observed' reflections ($I > 2\sigma_I$)	20023
Structure determined by:	dual methods, in SHELXT
Refinement:	Full-matrix least-squares on F^2, in SHELXL
Data / restraints / parameters	22692 / 1 / 1508
Goodness-of-fit on F^2	1.024
Final R indices ('observed' data)	R_1 = 0.049, wR_2 = 0.109
Final R indices (all data)	R_1 = 0.059, wR_2 = 0.113
Reflections weighted:	
$w = [\sigma^2(Fo^2)+(0.0444P)^2+21.29P]^{-1}$ where $P=(Fo^2+2Fc^2)/3$	
Absolute structure parameter	0.112(6)
Extinction coefficient	n/a
Largest diff. peak and hole	0.86 and -0.86 e.$Å^{-3}$

Location of largest difference peak near Zr(3)

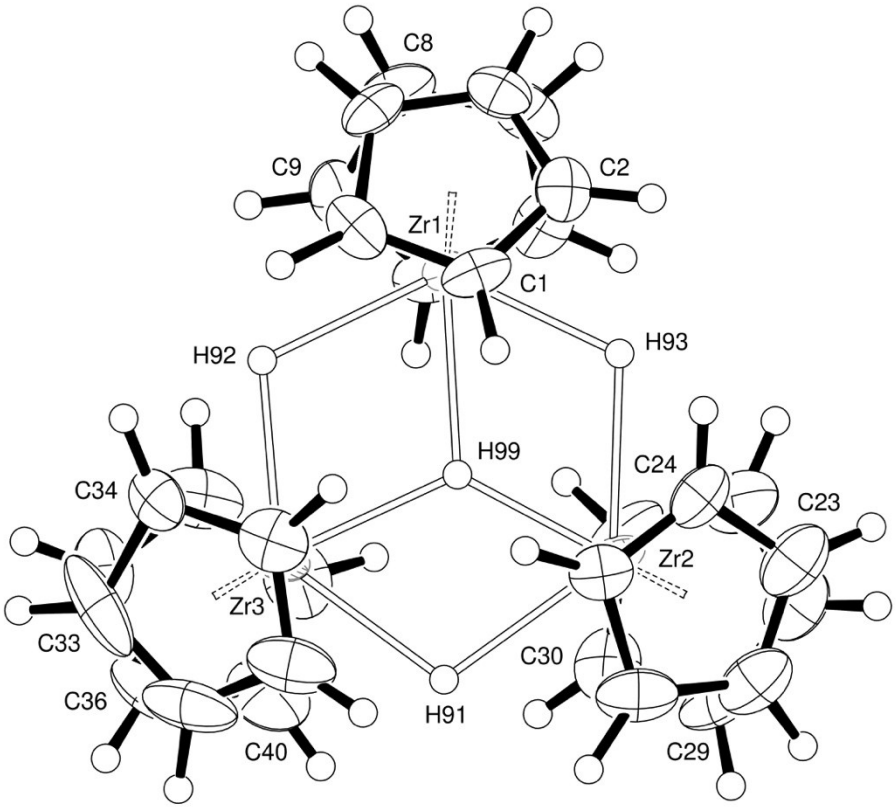

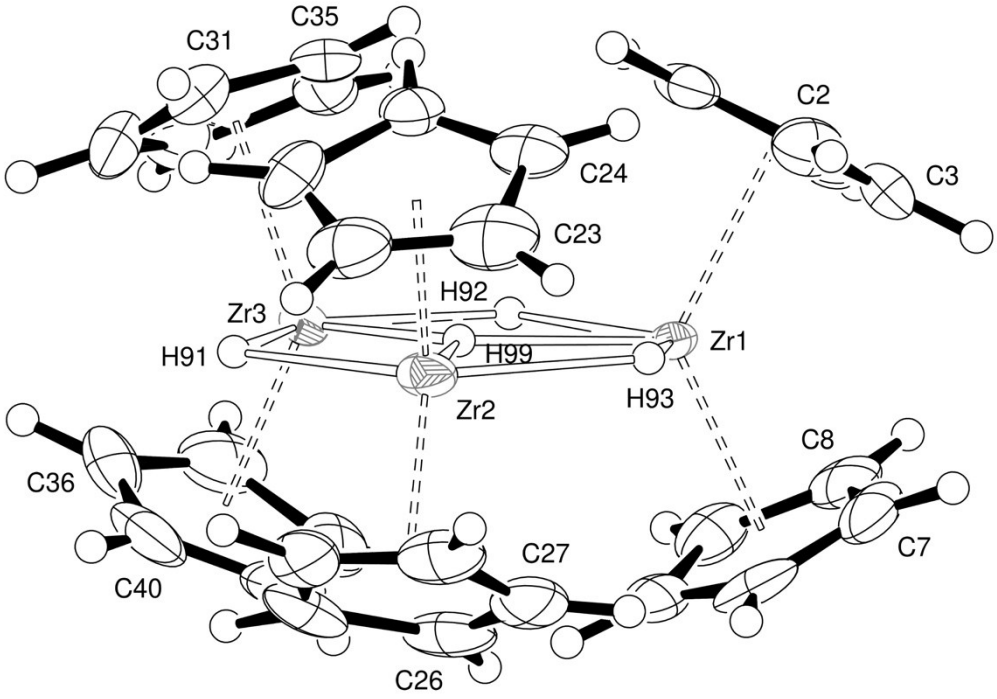

Figure S9. Two views of the $H(Cp_2ZrH)_3$ cation, indicating the atom numbering scheme. Thermal ellipsoids are drawn at the 50% probability level.

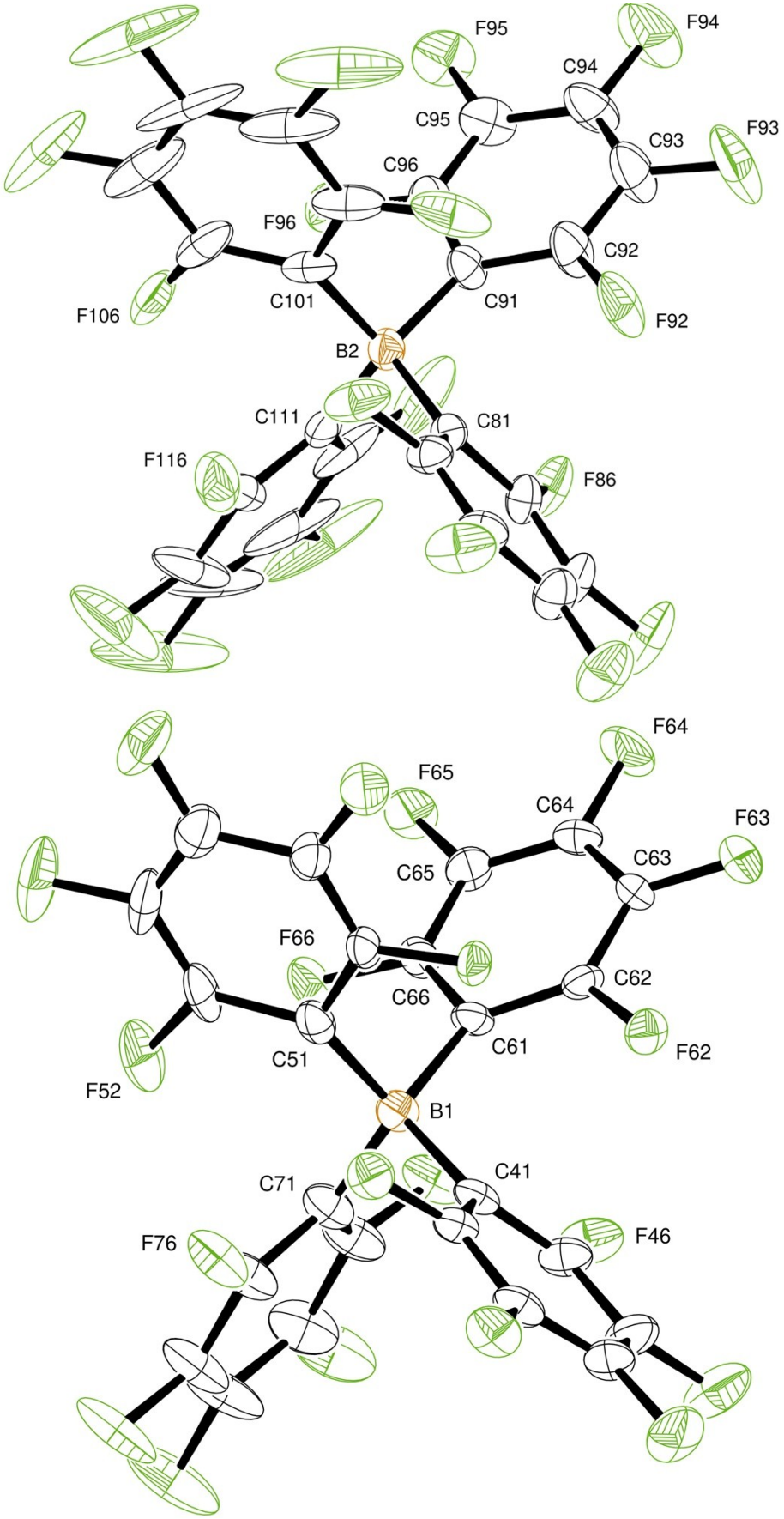

Figure S10. Views of the two $B(C_6F_5)_4$ anions.

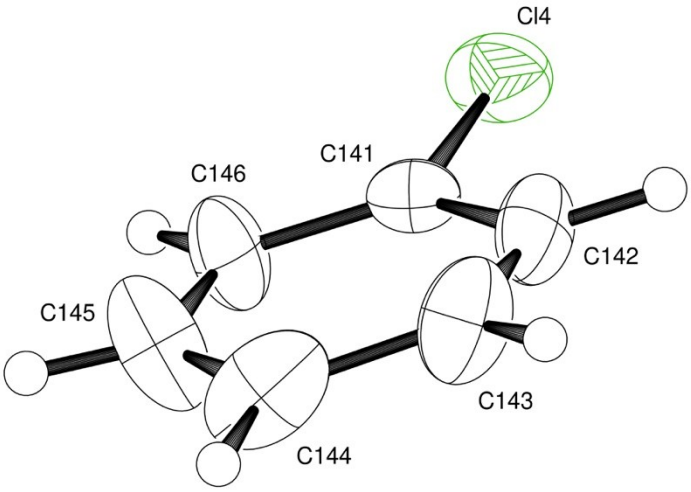

Figure S11. View of one of the more ordered solvent molecules.

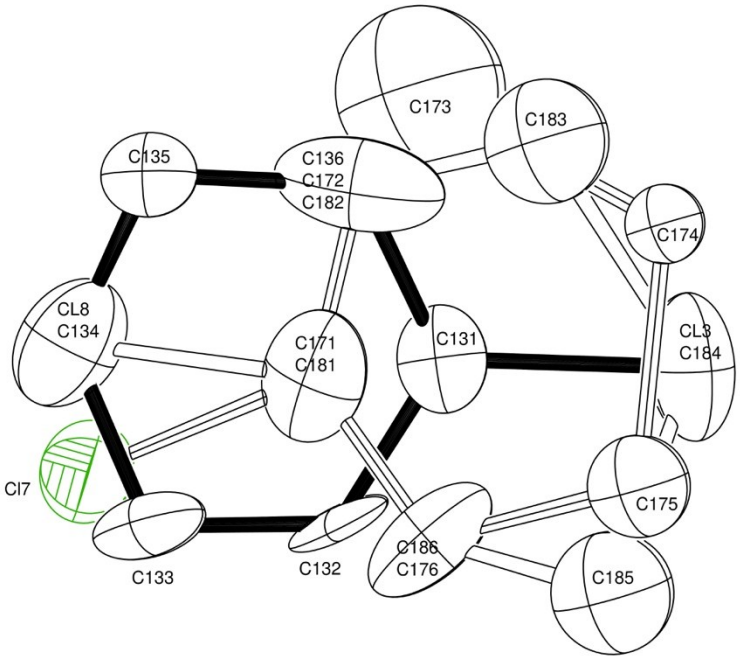

Figure S12. View of the disordered solvent molecules of Cl(3), Cl(7) and Cl(8) which are overlaid in a single unit. Note that Cl(8) occupies the same site as C(134) and Cl(3) as C(184); also that C(136), C(172) and C(182) share the same site (and thermal parameters), as do the pairs of C(171) and C(181), C(176) and C(186).

4. Computational methods

Geometries were optimized at the TPSSh[1]/Def2-SVP[2, 3] level using Turbomole[4] coupled to the external Baker optimizer.[5, 6] Vibrational analyses confirmed the nature of all stationay points as minima or transition states. IRC calculations were run from each heterolytic cleavage TS (in both directions) using Gaussian16[7] in order to establish connections to reactants and products (but see comments below). Final single-point energies were calculated with a PCM[8-10](chlorobenzene) solvent correctiont, the dispersion-including M062X functional[11, 12] and the cc-pVTZ basis set[13-15] (retrieved from the EMSL basiset exchange library[16, 17]) using Gaussian16.[7] These energies were combined with thermal corrections (enthalpy and entropy, 298 K, 1 bar) from the TPSSh/Def2-SVP vibrational analyses to arrive at the free energies mentioned in the text. Entropy corrections were scaled by a factor of 0.67 to acount for reduced freedom in solution.[18, 19]

Since these reactions involve developing charge separation in the H_2 molecule, solvent polarity was expected to be important. Therefore we also attempted to re-optimize all structures with inclusion of the PCM(chlorobenzene) solvent correction, still at the TPSSh/Def2-SVP level (using Gaussian16[7]). This worked for most stationary points but mostly not for the important H_2 cleavage transition states. The original PES is very flat near these transition states, and inclusion of the PCM correction introduces some artificial corrugation which causes even the otherwise extremely stable Baker optimizer to lose its way and either not converge at all or converge to spurious "stationary points" with small imaginary frequencies and corresponding meaningless modes. Numerous restarts from tweaked starting geometries did not help. For the remainder of the PES the differences in final energies due to in-solvent optimization were small (of the order of 1 kcal/mol for most stationary points). Therefore, we only cite in the text values derived from gas phase optimization.

A note on IRC runs:

As mentioned above, IRC calculations were run from each heterolytic cleavage TS (in both directions) in order to establish connections to reactats and products. The PES is very flat both around the TS (movement of H_2 relative to Cp_2ZrH^+/NR_3) and at the reactant/product stages (drifting away/recapture of NR_3 and drifting away/capture of H_2), causing many IRC runs to fail especially for the floppy $PhNMe_2$ system. Using larger or smaller stepsizes did not solve the problem. The only way to get completed IRC runs was to use a large stepsize (30 or more) ***and*** suppress the corrector step (ReCorrect=Never), which might result in unreliable paths. Therefore, we also tested each connection by moving each TS along the reaction coordinate (in both directions, 0.03 to 0.20 bohr) and re-optimizing. While this cannot produce an ideal IRC path, it does prove that there is a "downhill-only" connection between the TS and its reactants/products.

A note on naming:

Species are labeled **A**-**K** as illustrated in the following figures. The first (lowercase) letter of the name indicates the system (the base used): "**n**" for $PhNMe_2$, "**m**" for NMe_3, "**e**" for $MeNEt_2$, "**p**" for PMe_3, "**a**" for the $Cp_2Zr(OPh)(NMe_3)^+$ system, and "**z**" for species that are not base-specific. Thus, **mE+** stands for NMe_3 system, species **E**. Transition states (shown in blue in the figures) have "**TS**" in the name, followed by letters indicating the connected species. Thus, **nTS_DE+** is (in the $PhNMe_2$ system) the TS connecting species **D** and **E**. Lowercase letters abc.. near the end of a name indicate separate conformers, usually close in energy to each other.

Reaction paths for $PhNMe_2$

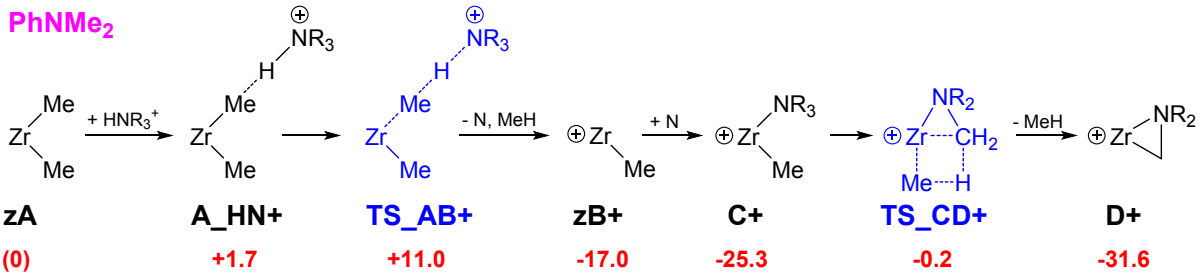

Figure S13. $PhNMe_2$: formation of metalla-aziridine.

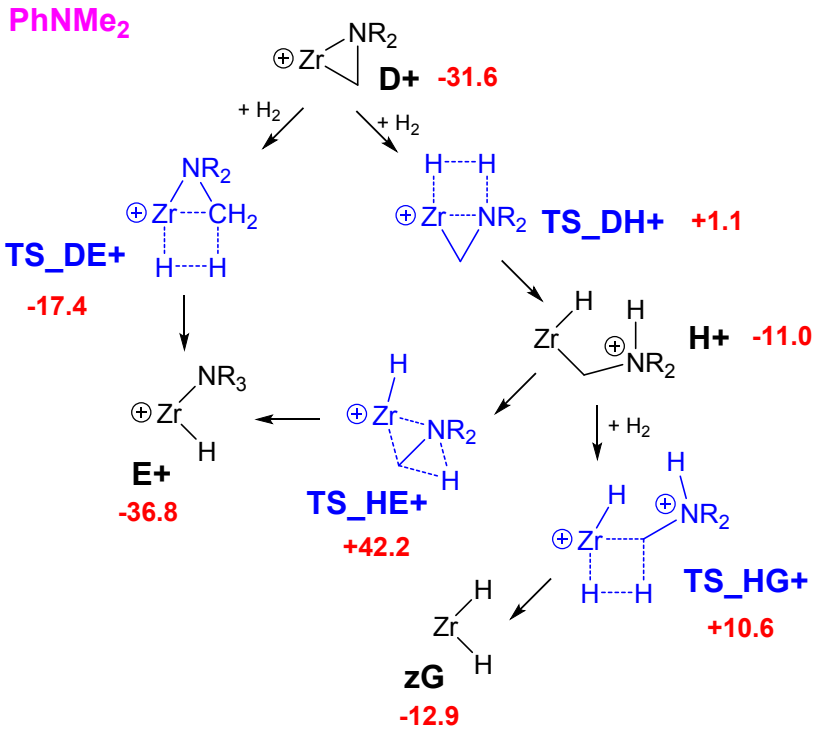

Figure S14. $PhNMe_2$: hydrogenolysis of metalla-aziridine.

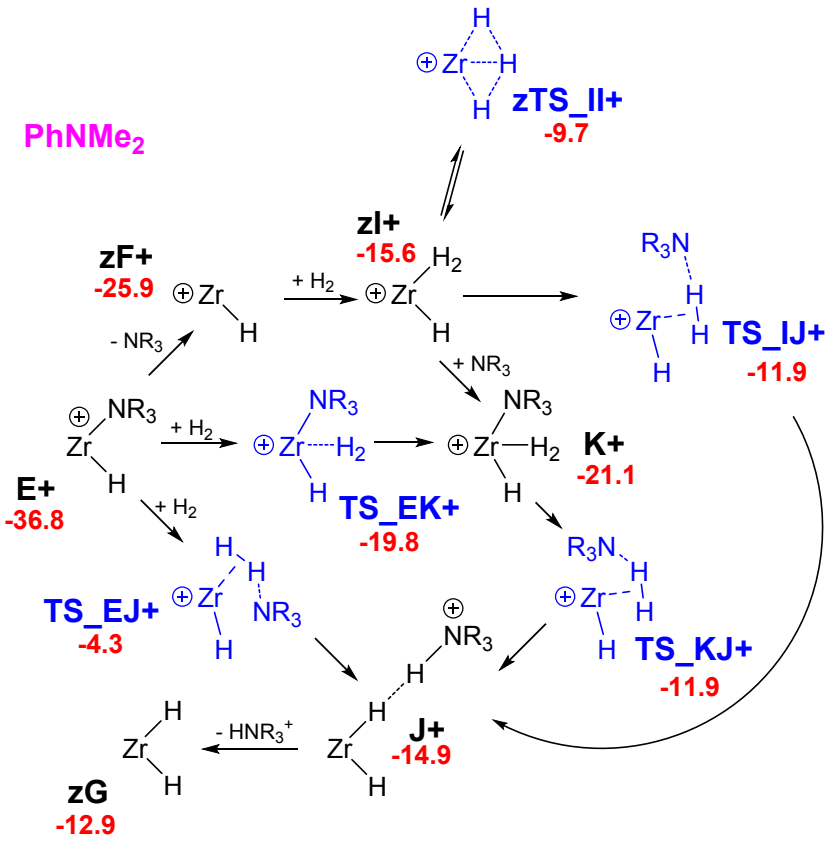

Figure S15. $PhNMe_2$: heterolytic H_2 cleavage.

Table S1. Free energies for $PhNMe_2$ reactions.[a]

Name	Formula	Hcorr	TScorr	Eelec	G	on scale	rel
zH2	H2	0.01333	0.01556	-1.16882	-1.16592		
zCH4	CH4	0.04853	0.02114	-40.50122	-40.46685		
nPhNMe2	C8H11N	0.18261	0.04382	-366.17957	-366.02632		
nPhNMe2H+	C8H12N	0.19738	0.04291	-366.60827	-366.43964		
nPhNMe22H+	C16H23N2	0.38160	0.06869	-732.80590	-732.47033		
zA	C12H16Zr	0.25302	0.05665	-513.75994	-513.54488	-513.54488	(0)
nA_HN+	C20H28NZr	0.45196	0.08570	-880.37884	-879.98430	-513.54466	0.14
nTS_AB+	C20H28NZr	0.44673	0.08345	-880.36063	-879.96981	-513.53017	9.23
nB+_N	C19H24NZr	0.40209	0.07396	-839.90360	-839.55107	-513.57828	-20.96
zB+	C11H13Zr	0.21621	0.05319	-473.69644	-473.51586	-513.56939	-15.38
nCa+	C19H24NZr	0.40263	0.07187	-839.91437	-839.55989	-513.58710	-26.49
nCb+	C19H24NZr	0.40255	0.07265	-839.91294	-839.55906	-513.58627	-25.97
nTS_CD+	C19H24NZr	0.39799	0.06881	-839.87088	-839.51900	-513.54621	-0.83
nD+	C18H20NZr	0.35124	0.06625	-799.40659	-799.09974	-513.59380	-30.70
nTS_DE+	C18H22NZr	0.36742	0.06575	-800.56711	-800.24374	-513.57189	-16.95
nEa+	C18H22NZr	0.37241	0.06657	-800.59986	-800.27205	-513.60020	-34.71
nEb+	C18H22NZr	0.37219	0.06721	-800.60172	-800.27457	-513.60271	-36.29
nTS_DH+	C18H22NZr	0.36644	0.06819	-800.53700	-800.21625	-513.54440	0.30

Name	Formula	Hcorr	TScorr	Eelec	G	on scale	rel
nH+	C18H22NZr	0.37126	0.07242	-800.55746	-800.23472	-513.56287	-11.29
nTS_HEa+	C18H22NZr	0.36469	0.07213	-800.46749	-800.15113	-513.47927	41.17
nTS_HEb+	C18H22NZr	0.36463	0.07065	-800.46640	-800.14910	-513.47724	42.44
nTS_HEc+	C18H22NZr	0.36456	0.07123	-800.46598	-800.14915	-513.47729	42.41
nTS_HGa+	C18H24NZr	0.38694	0.07208	-801.69901	-801.36036	-513.52258	13.99
nTS_HGb+	C18H24NZr	0.38729	0.07024	-801.70430	-801.36407	-513.52630	11.66
zG	C10H12Zr	0.19203	0.04794	-435.12414	-434.96423	-513.56609	-13.31
zF+	C10H11Zr	0.18618	0.04722	-434.38390	-434.22936	-513.58383	-24.44
zIa+	C10H13Zr	0.20329	0.04903	-435.55093	-435.38049	-513.56904	-15.16
zIb+	C10H13Zr	0.20268	0.05028	-435.54981	-435.38083	-513.56937	-15.37
zTS_II+	C10H13Zr	0.20099	0.04870	-435.53951	-435.37115	-513.55970	-9.30
nTS_EKa+	C18H24NZr	0.38773	0.06877	-801.75784	-801.41619	-513.57841	-21.04
nTS_EKb+	C18H24NZr	0.38752	0.06894	-801.75668	-801.41536	-513.57758	-20.52
nKa+	C18H24NZr	0.38989	0.06906	-801.76028	-801.41666	-513.57888	-21.33
nKb+	C18H24NZr	0.39016	0.06829	-801.75795	-801.41354	-513.57576	-19.37
nTS_KJvb+	C18H24NZr	0.38681	0.07541	-801.73396	-801.39768	-513.55990	-9.42
nTS_KJwap+	C18H24NZr	0.38672	0.07588	-801.73440	-801.39852	-513.56074	-9.95
nTS_EJa+	C18H24NZr	0.38768	0.07318	-801.73704	-801.39839	-513.56062	-9.87
nTS_EJb+	C18H24NZr	0.38746	0.07442	-801.73422	-801.39662	-513.55884	-8.76
nTS_EJc+	C18H24NZr	0.38759	0.07388	-801.73798	-801.39989	-513.56211	-10.81
nTS_IJua+	C18H24NZr	0.38603	0.07294	-801.73779	-801.40063	-513.56285	-11.27
nTS_IJub+	C18H24NZr	0.38595	0.07285	-801.73770	-801.40055	-513.56277	-11.23
nTS_IJvap+	C18H24NZr	0.38608	0.07311	-801.73890	-801.40181	-513.56403	-12.01
nJa+	C18H24NZr	0.39016	0.07798	-801.74794	-801.41003	-513.57225	-17.17
nJb+	C18H24NZr	0.39027	0.07782	-801.74798	-801.40985	-513.57207	-17.06
zG	C10H12Zr	0.19203	0.04794	-435.12414	-434.96423	-513.56609	-13.31

[a] Geometries optimized, thermal corrections at TPSSh/Def2-SVP (298 K, 1 bar). Electronic energies at PCM(chlorobenzene)/M06-2X/cc-pVTZ. Free energies calculated as $E_{elec} + H_{corr} - 0.67\ TS_{corr}$.

Reaction paths for NMe_3

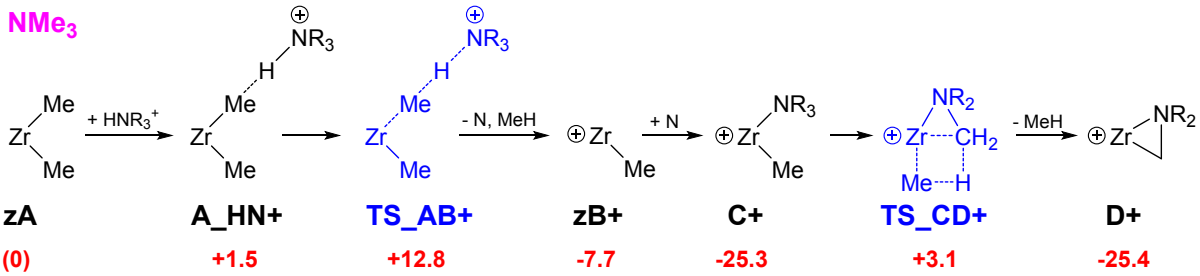

Figure S16. NMe_3: formation of metalla-aziridine.

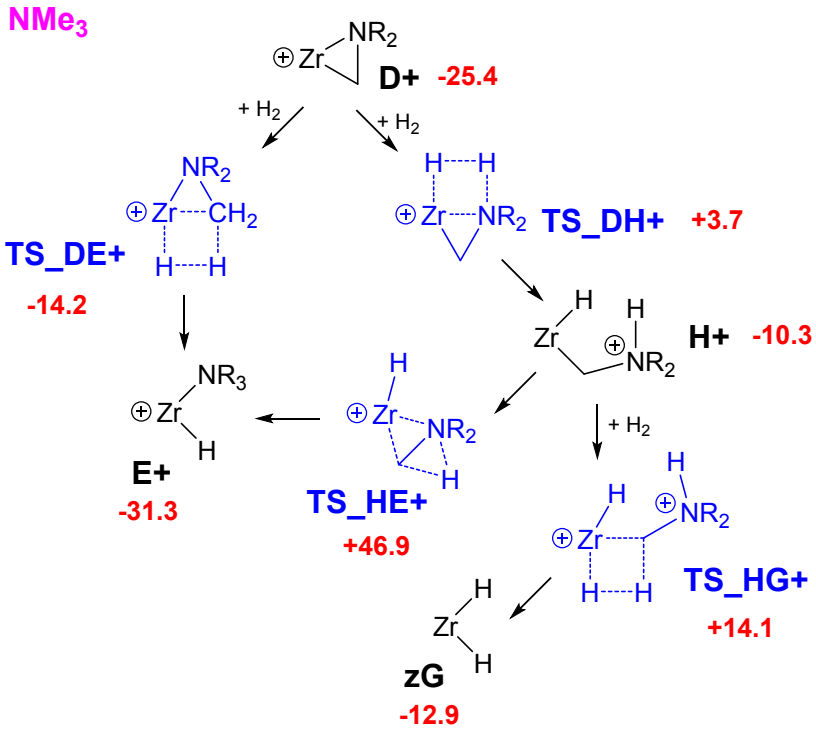

Figure S17. NMe_3: hydrogenolysis of metalla-aziridine.

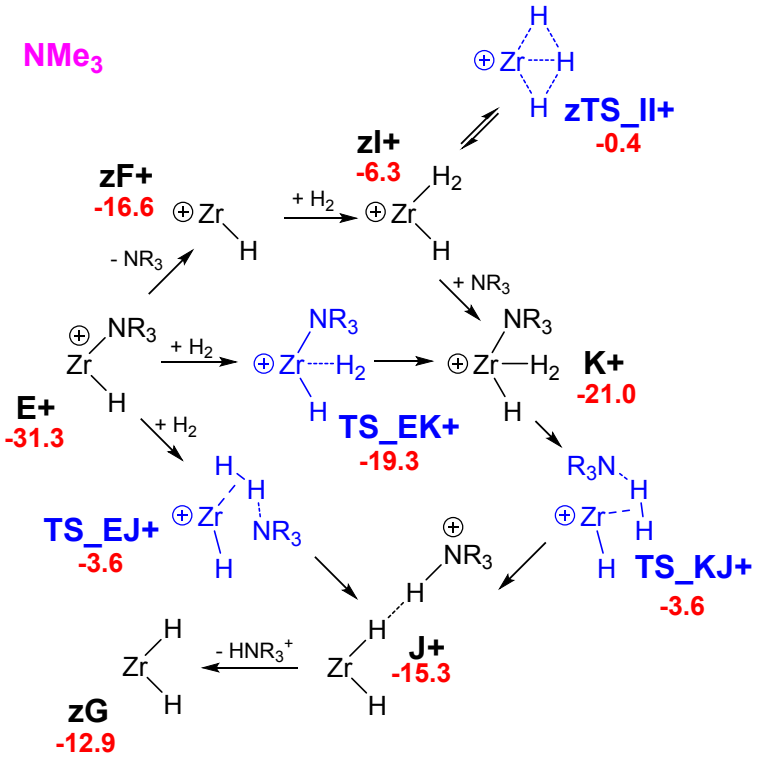

Figure S18. NMe_3: heterolytic H_2 cleavage.

Table S2. Free energies for NMe_3 reactions.[a]

Name	Formula	Hcorr	TScorr	Eelec	G	on scale	rel
zH2	H2	0.01333	0.01556	-1.16882	-1.16592		
zCH4	CH4	0.04853	0.02114	-40.50122	-40.46685		
mNMe3	C3H9N	0.12615	0.03388	-174.44466	-174.34121		
mNMe3H+	C3H10N	0.14218	0.03425	-174.88868	-174.76944		
mMe3N2H+	C6H19N2	0.26921	0.05192	-349.35700	-349.12257		
zA	C12H16Zr	0.25302	0.05665	-513.75994	-513.54488	-513.54488	(0)
mA_HN+	C15H26NZr	0.39643	0.07821	-688.65770	-688.31367	-513.54422	0.41
mTS_AB+	C15H26NZr	0.39099	0.07652	-688.63664	-688.29691	-513.52747	10.93
zB+	C11H13Zr	0.21621	0.05319	-473.69644	-473.51586	-513.55449	-6.03
mCa+	C14H22NZr	0.34646	0.06447	-648.19141	-647.88815	-513.58556	-25.53
mCb+	C14H22NZr	0.34652	0.06437	-648.19146	-647.88807	-513.58549	-25.48
mTS_CD+	C14H22NZr	0.34288	0.06020	-648.14470	-647.84215	-513.53957	3.34
mD+	C13H18NZr	0.29582	0.05866	-607.67648	-607.41996	-513.58423	-24.69
mTS_DE+	C13H20NZr	0.31215	0.05672	-608.84154	-608.56739	-513.56574	-13.09
mE+	C13H20NZr	0.31591	0.06186	-608.87196	-608.59749	-513.59584	-31.98
mTS_DH+	C13H20NZr	0.31096	0.05976	-608.81202	-608.54109	-513.53944	3.42
mH+	C13H20NZr	0.31603	0.06296	-608.83686	-608.56301	-513.56136	-10.34
mTS_HEa+	C13H20NZr	0.30877	0.06331	-608.73737	-608.47101	-513.46936	47.39
mTS_HEb+	C13H20NZr	0.30878	0.06308	-608.73710	-608.47058	-513.46892	47.67
mTS_HGa+	C13H22NZr	0.33178	0.06263	-609.97848	-609.68866	-513.52108	14.93
mTS_HGb+	C13H22NZr	0.33183	0.06222	-609.97991	-609.68977	-513.52219	14.24

Name	Formula	Hcorr	TScorr	Eelec	G	on scale	rel
zG	C10H12Zr	0.19203	0.04794	-435.12414	-434.96423	-513.56609	-13.31
zF+	C10H11Zr	0.18618	0.04722	-434.38390	-434.22936	-513.56892	-15.09
zIa+	C10H13Zr	0.20329	0.04903	-435.55093	-435.38049	-513.55413	-5.80
zIb+	C10H13Zr	0.20268	0.05028	-435.54981	-435.38083	-513.55446	-6.01
zTS_II+	C10H13Zr	0.20099	0.04870	-435.53951	-435.37115	-513.54479	0.06
mTS_EK+	C13H22NZr	0.33143	0.06326	-610.03681	-609.74776	-513.58018	-22.15
mK+	C13H22NZr	0.33402	0.06041	-610.03896	-609.74541	-513.57783	-20.68
mTS_KJ+	C13H22NZr	0.33120	0.06770	-610.00515	-609.71930	-513.55172	-4.29
mTS_EJ+	C13H22NZr	0.33181	0.06564	-610.00808	-609.72026	-513.55268	-4.89
mJ+	C13H22NZr	0.33474	0.07020	-610.02864	-609.74093	-513.57335	-17.86
zG	C10H12Zr	0.19203	0.04794	-435.12414	-434.96423	-513.56609	-13.31

[a] Geometries optimized, thermal corrections at TPSSh/Def2-SVP (298 K, 1 bar). Electronic energies at PCM(chlorobenzene)/M06-2X/cc-pVTZ. Free energies calculated as E_{elec} + H_{corr} - 0.67 TS_{corr}.

Table S3. Free energies for $MeNEt_2$ coordination.[a]

Name	Formula	Hcorr	TScorr	Eelec	G	on scale	rel
eMeNEt2_a	C5H13N	0.18550	0.04102	-253.05944	-252.90143		
eMeNEt2_b	C5H13N	0.18545	0.04147	-253.06034	-252.90267		
eMeNEt2H+_a	C5H14N	0.20137	0.04110	-253.50661	-253.33277		
eMeNEt2H+_b	C5H14N	0.20121	0.04184	-253.50680	-253.33363		
eEa+	C15H24NZr	0.37592	0.06491	-687.48106	-687.14863	-687.14863	0.05
eEb+	C15H24NZr	0.37598	0.06507	-687.48110	-687.14872	-687.14872	(0)
eEc+	C15H24NZr	0.37537	0.06611	-687.47947	-687.14839	-687.14839	0.21
zF+	C10H11Zr	0.18618	0.04722	-434.38390	-434.22936	-687.13204	10.47

[a] Geometries optimized, thermal corrections at TPSSh/Def2-SVP (298 K, 1 bar). Electronic energies at PCM(chlorobenzene)/M06-2X/cc-pVTZ. Free energies calculated as E_{elec} + H_{corr} - 0.67 TS_{corr}.

Reaction paths for PMe_3

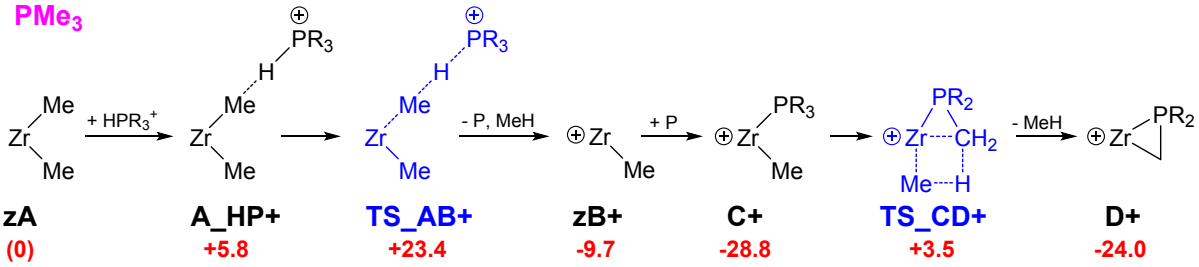

Figure S19. PMe_3: metalla-phosphorane formation.

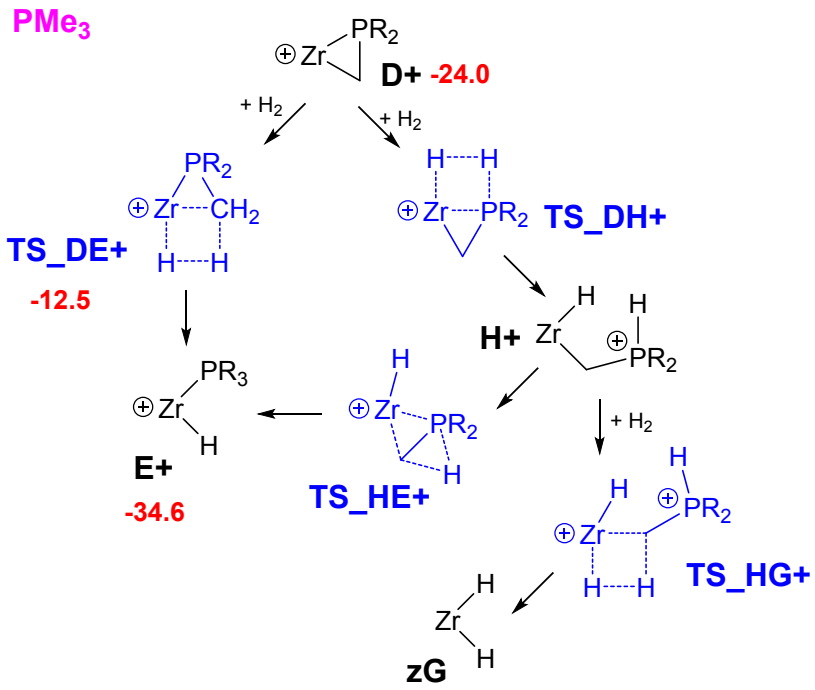

Figure S20. PMe_3: hydrogenolysis of metalla-phosphorane.

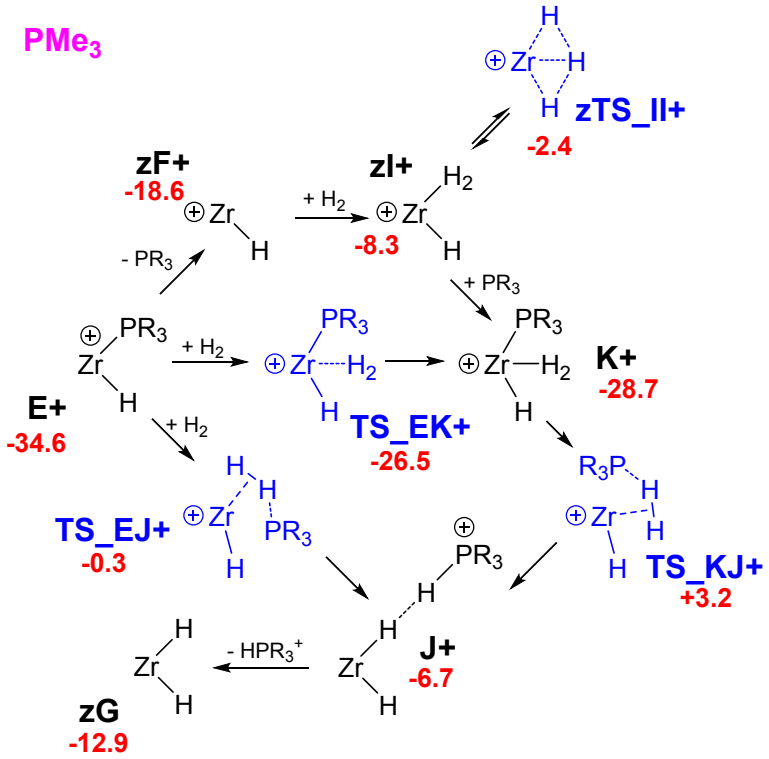

Figure S21. PMe_3: heterolytic H_2 cleavage.

Table S4. Free energies for PMe_3 reactions.[a]

Name	Formula	Hcorr	TScorr	Eelec	G	on scale	rel
zH2	H2	0.01333	0.01556	-1.16882	-1.16592		
zCH4	CH4	0.04853	0.02114	-40.50122	-40.46685		
pPMe3	C3H9P	0.11974	0.03702	-461.06899	-460.97406		
pPMe3H+	C3H10P	0.13105	0.03731	-461.50465	-461.39860		
pMe3P2H+	C6H19P2	0.25244	0.06240	-922.57645	-922.36582		
zA	C12H16Zr	0.25302	0.05665	-513.75994	-513.54488	-513.54488	(0)
pA_HP+	C15H26PZr	0.38567	0.08311	-975.26652	-974.93654	-513.53794	4.36
pTS_AB+	C15H26PZr	0.38208	0.08040	-975.23716	-974.90894	-513.51034	21.67
zB+	C11H13Zr	0.21621	0.05319	-473.69644	-473.51586	-513.55817	-8.34
pCa+	C14H22PZr	0.33883	0.06972	-934.81576	-934.52364	-513.59190	-29.50
pCb+	C14H22PZr	0.33883	0.06971	-934.81615	-934.52403	-513.59229	-29.75
pTS_CD+	C14H22PZr	0.33535	0.06436	-934.76370	-934.47147	-513.53972	3.24
pD+	C13H18PZr	0.28875	0.06258	-894.29459	-894.04776	-513.58287	-23.83
pTS_DE+	C13H20PZr	0.30485	0.06087	-895.45927	-895.19520	-513.56438	-12.24
pE+	C13H20PZr	0.30860	0.06727	-895.49626	-895.23273	-513.60191	-35.79
zF+	C10H11Zr	0.18618	0.04722	-434.38390	-434.22936	-513.57260	-17.40
zIa+	C10H13Zr	0.20329	0.04903	-435.55093	-435.38049	-513.55781	-8.11
zIb+	C10H13Zr	0.20268	0.05028	-435.54981	-435.38083	-513.55814	-8.32
zTS_II+	C10H13Zr	0.20099	0.04870	-435.53951	-435.37115	-513.54847	-2.25
pTS_EK+	C13H22PZr	0.32325	0.06934	-896.66595	-896.38916	-513.59242	-29.83
pK+	C13H22PZr	0.32642	0.06445	-896.68251	-896.39928	-513.60254	-36.18

Name	Formula	Hcorr	TScorr	Eelec	G	on scale	rel
pTS_KJ+	C13H22PZr	0.32286	0.07375	-896.61733	-896.34388	-513.54714	-1.42
pTS_EJ+	C13H22PZr	0.32279	0.06703	-896.62627	-896.34839	-513.55165	-4.25
pJ+	C13H22PZr	0.32416	0.07258	-896.63582	-896.36029	-513.56356	-11.72
zG	C10H12Zr	0.19203	0.04794	-435.12414	-434.96423	-513.56609	-13.31

[a] Geometries optimized, thermal corrections at TPSSh/Def2-SVP (298 K, 1 bar). Electronic energies at PCM(chlorobenzene)/M06-2X/cc-pVTZ. Free energies calculated as $E_{elec} + H_{corr} - 0.67\ TS_{corr}$.

Reaction paths for $Cp_2Zr(OPh)(NMe_3)^+$

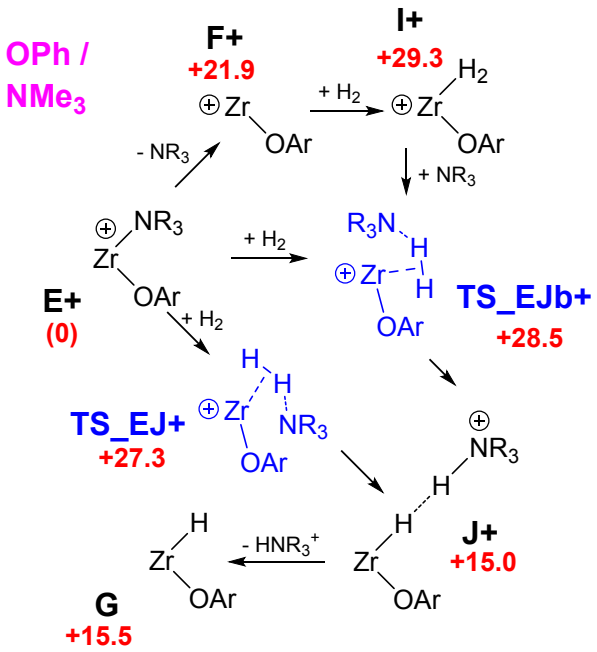

Figure S22. $Cp_2Zr(OPh)(NMe_3)^+$: heterolytic H_2 cleavage.

Table S5. Free energies for $Cp_2Zr(OPh)(NMe_3)^+$ reactions.[a]

Name	Formula	Hcorr	TScorr	Eelec	G	on scale	rel
zH2	H2	0.01333	0.01556	-1.16882	-1.16592		
mNMe3	C3H9N	0.12615	0.03388	-174.44466	-174.34121		
mNMe3H+	C3H10N	0.14218	0.03425	-174.88868	-174.76944		
aE+	C19H24NOZr	0.41011	0.07611	-915.21321	-914.85410	-914.85410	(0)
aF+	C16H15OZr	0.27980	0.06574	-740.71487	-740.47912	-914.82033	21.19
aI+	C16H17OZr	0.29682	0.06679	-741.88591	-741.63384	-914.80913	28.22
aTS_EJ+	C19H26NOZr	0.42605	0.07933	-916.34804	-915.97514	-914.80922	28.16
aTS_EJc+	C19H26NOZr	0.42519	0.07923	-916.34509	-915.97299	-914.80706	29.51
aJ+	C19H26NOZr	0.42958	0.08284	-916.37212	-915.99804	-914.83212	13.79
aG	C16H16OZr	0.28658	0.06644	-741.46727	-741.22520	-914.82872	15.92

[a] Geometries optimized, thermal corrections at TPSSh/Def2-SVP (298 K, 1 bar). Electronic energies at PCM(chlorobenzene)/M06-2X/cc-pVTZ. Free energies calculated as $E_{elec} + H_{corr} - 0.67\ TS_{corr}$.

Formation of $Cp_6Zr_3H_4^{2+}$

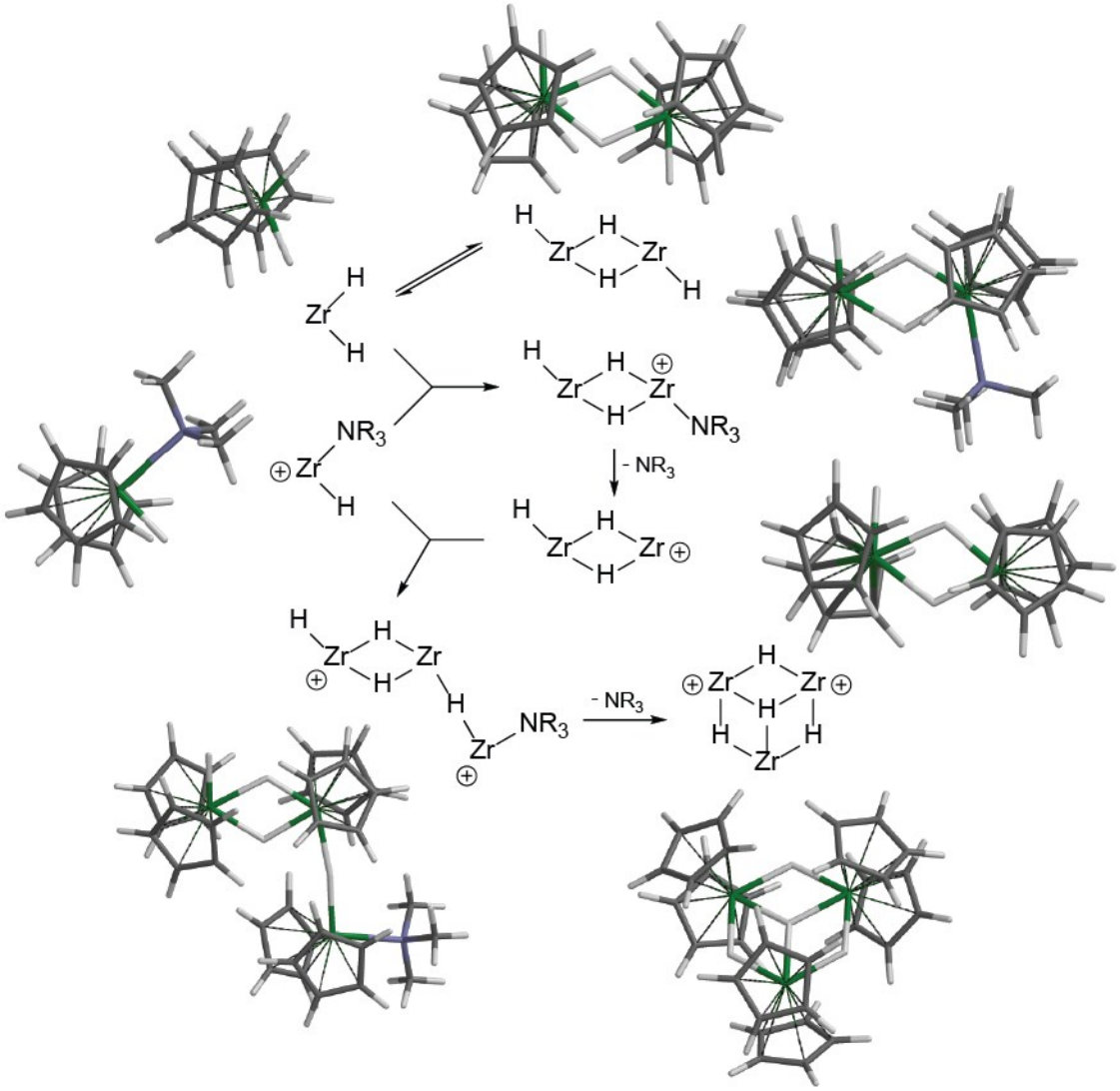

Figure S23. Plausible steps in formation of trinuclear cluster.

Table S6. Free energies for plausible species in cluster formation.[a]

Name	Formula	Hcorr	TScorr	Eelec	G
For NMe_3					
zH2	H2	0.01333	0.01556	-1.16882	-1.16592
mNMe3	C3H9N	0.12615	0.03388	-174.44466	-174.34121
mNMe3H+	C3H10N	0.14218	0.03425	-174.88868	-174.76944
mMe3N2H+	C6H19N2	0.26921	0.05192	-349.35700	-349.12257
zG	C10H12Zr	0.19203	0.04794	-435.12414	-434.96423
zZr2H4	C20H24Zr2	0.38894	0.07244	-870.30580	-869.96539
mE+	C13H20NZr	0.31591	0.06186	-608.87196	-608.59749
mZr2H3_+_N	C23H32NZr2	0.51273	0.08540	-1044.04943	-1043.59392
zZr2H3_+	C20H23Zr2	0.38201	0.07311	-869.56330	-869.23027
mZr3H4_2+_N	C33H43NZr3	0.69993	0.11291	-1478.44568	-1477.82141
zZr3H4_2+	C30H34Zr3	0.57225	0.09189	-1304.00538	-1303.49470
For $PhNMe_2$					
nPhNMe2	C8H11N	0.18261	0.04382	-366.17957	-366.02632
nPhNMe2H+	C8H12N	0.19738	0.04291	-366.60827	-366.43964
nPhNMe22H+	C16H23N2	0.38160	0.06869	-732.80590	-732.47033
nEb+	C18H22NZr	0.37219	0.06721	-800.60172	-800.27457
For $MeNEt_2$					
eMeNEt2_b	C5H13N	0.18545	0.04147	-253.06034	-252.90267
eMeNEt2H+_b	C5H14N	0.20121	0.04184	-253.50680	-253.33363
eMeNEt22H+	C10H27N2	0.38846	0.06395	-506.58864	-506.24302
eEb+	C15H24NZr	0.37598	0.06507	-687.48110	-687.14872

[a] Geometries optimized, thermal corrections at TPSSh/Def2-SVP (298 K, 1 bar). Electronic energies at PCM(chlorobenzene)/M06-2X/cc-pVTZ. Free energies calculated as $E_{elec} + H_{corr} - 0.67\ TS_{corr}$.

Table S7. Free energy changes for plausible steps in cluster formation.[a]

Reactants	Products	ΔG
For NMe_3:		
$Cp_2ZrH(NR_3)^+$	$Cp_2ZrH^+ + NR_3$	16.89
$Cp_2ZrH(NR_3) + H_2$	$Cp_2ZrH_2 + HNR_3^+$	18.67
$2\ Cp_2ZrH_2$	$Cp_4Zr_2H_4$	-23.18
$Cp_2ZrH_2 + Cp_2ZrH(NR_3)^+$	$Cp_4Zr_2H_3(NR_3)^+$	-20.20
$Cp_4Zr_2H_3(NR_3)^+$	$Cp_4Zr_2H_3^+ + NR_3$	14.08
$Cp_4Zr_2H_3^+ + Cp_2ZrH(NR_3)^+$	$Cp_6Zr_3H_4(NR_3)^{2+}$	3.99
$Cp_6Zr_3H_4(NR_3)^{2+}$	$Cp_6Zr_3H_4^{2+} + NR_3$	-9.10
$3\ Cp_2ZrH(NR_3)^+ + H_2$	$Cp_6Zr_3H_4^{2+} + 2\ NR_3 + HNR_3^+$	7.43
$3\ Cp_2ZrH(NR_3)^+ + H_2$	***$Cp_6Zr_3H_4^{2+} + NR_3 + H[NR_3]_2^+$***	***-0.05***
For $PhNMe_2$:		
$Cp_2ZrH(NR_3)^+$	$Cp_2ZrH^+ + NR_3$	11.85
$3\ Cp_2ZrH(NR_3)^+ + H_2$	$Cp_6Zr_3H_4^{2+} + 2\ NR_3 + HNR_3^+$	1.65
$3\ Cp_2ZrH(NR_3)^+ + H_2$	***$Cp_6Zr_3H_4^{2+} + NR_3 + H[NR_3]_2^+$***	***-1.08***
For $MeNEt_2$:		
$Cp_2ZrH(NR_3)^+$	$Cp_2ZrH^+ + NR_3$	10.47
$3\ Cp_2ZrH(NR_3)^+ + H_2$	$Cp_6Zr_3H_4^{2+} + 2\ NR_3 + HNR_3^+$	-13.55
$3\ Cp_2ZrH(NR_3)^+ + H_2$	***$Cp_6Zr_3H_4^{2+} + NR_3 + H[NR_3]_2^+$***	***-17.77***
For PMe_3:		
$Cp_2ZrH(PR_3)^+$	$Cp_2ZrH^+ + PR_3$	18.39
$3\ Cp_2ZrH(PR_3)^+ + H_2$	***$Cp_6Zr_3H_4^{2+} + 2\ PR_3 + HPR_3^+$***	***14.24***
$3\ Cp_2ZrH(PR_3)^+ + H_2$	$Cp_6Zr_3H_4^{2+} + PR_3 + H[PR_3]_2^+$	18.53

[a] Based on free energies listed in Table S6.

Discussion: cluster formation.

Assuming the reaction stoichiometry

$$3\ Cp_2ZrH(NR_3)^+ + H_2 \rightarrow Cp_6Zr_3H_4^{2+} + 2\ NR_3 + HNR_3^+$$

the free energy change as a function of the base (amine/phosphine) depends mainly on the coordination energy of the base to the Cp_2ZrH^+ fragment (this is the first reaction listed for each base in Table S7 above). For $PhNMe_2$ (coordination energy 11.85 kcal/mol) the cluster formation reaction is predicted to be *endergonic* by 1.65 kcal/mol. However, in solution (in a non-protic solvent) the acid produced (HNR_3^+) is likely to stay associated with one equivalent of base:

$$3\ Cp_2ZrH(NR_3)^+ + H_2 \rightarrow Cp_6Zr_3H_4^{2+} + NR_3 + H[NR_3]_2^+$$

When corrected for this (included in Table S7), cluster formation becomes barely (-1.08 kcal/mol) exergonic. NMe_3 coordinates more strongly (16.89 kcal/mol) but also forms a stronger acid-base pair, and cluster formation stays barely exergonic (-0.05 kcal/mol). $MeNEt_2$ (as a better model for $MeNHx_2$) coordinates more weakly (10.47 kcal/mol; presumably for steric reasons) and hence cluster formation becomes very favourable (-17.77 kcal/mol). For PMe_3 (coordination energy 18.39 kcal/mol) acid-base pairing doesn't help and cluster formation is significantly endergonic (+14.24 kcal/mol).

References

1) J. M. Tao, J. P. Perdew, V. N. Staroverov and G. E. Scuseria, *Phys. Rev. Lett.* 2003, **91**, 146401.
2) F. Weigend and R. Ahlrichs, *Phys. Chem. Chem. Phys.* 2005, **7**, 3297
3) K. Eichkorn, F. Weigend, O. Treutler and R. Ahlrichs, *Theor. Chem. Acc.* 1997, **97**, 119.
4) *TURBOMOLE*, V6.3; TURBOMOLE GmbH, since 2007: Karlsruhe, 2011.
5) J. Baker, *PQS*, 2.4; Parallel Quantum Solutions: Fayetteville, AR, 2001.
6) J. Baker, *J. Comput. Chem.* **1986,** *7* (4), 385-395.
7) M. J. Frisch, G. W. Trucks, H. B. Schlegel, G. E. Scuseria, M. A. Robb, J. R. Cheeseman, G. Scalmani, V. Barone, G. A. Petersson, H. Nakatsuji, X. Li, M. Caricato, A. V. Marenich, J. Bloino, B. G. Janesko, R. Gomperts, B. Mennucci, H. P. Hratchian, J. V. Ortiz, A. F. Izmaylov, J. L. Sonnenberg, D. Williams-Young, F. Ding, F. Lipparini, F. Egidi, J. Goings, B. Peng, A. Petrone, T. Henderson, D. Ranasinghe, V. G. Zakrzewski, J. Gao, N. Rega, G. Zheng, W. Liang, M. Hada, M. Ehara, K. Toyota, R. Fukuda, J. Hasegawa, M. Ishida, T. Nakajima, Y. Honda, O. Kitao, H. Nakai, T. Vreven, K. Throssell, J. A. Montgomery, Jr., J. E. Peralta, F. Ogliaro, M. J. Bearpark, J. J. Heyd, E. N. Brothers, K. N. Kudin, V. N. Staroverov, T. A. Keith, R. Kobayashi, J. Normand, K. Raghavachari, A. P. Rendell, J. C. Burant, S. S. Iyengar, J. Tomasi, M. Cossi, J. M. Millam, M. Klene, C. Adamo, R. Cammi, J. W. Ochterski, R. L. Martin, K. Morokuma, O. Farkas, J. B. Foresman and D. J. Fox, Gaussian 16, C.01, Gaussian, Inc.: Wallingford CT, 2016.
8) S. Miertuš and J. Tomasi, *Chem. Phys.* 1982, **65**, 239.
9) S. Miertuš, E. Scrocco and J. Tomasi, *Chem. Phys.* **1981,** *55* (1), 117-129.
10) G. Scalmani and M. J. Frisch, *J. Chem. Phys.* 2010, **132**, 114110
11) Y. Zhao and D. G. Truhlar, *Theor. Chem. Acc.* 2008, **120**, 215.
12) C. Ehm, P. H. M. Budzelaar and V. Busico, *J. Organomet. Chem.* 2015, **775**, 39.
13) T.H. Dunning, *J. Chem. Phys.* 1989, **90**, 1007.
14) D. E. Woon and T. H. Dunning, *J. Chem. Phys.* 1993, **98**, 1358.
15) K. A. Peterson, D. Figgen, M. Dolg and H. Stoll, *J. Chem. Phys.* 2007, **126**, 124101.
16) K. L. Schuchardt, B. T. Didier, T. Elsethagen, L.S. Sun, V. Gurumoorthi, J. Chase, J. Li and T. L. Windus, *J. Chem. Inf. Model.* 2007, **47**, 1045.
17) D. Feller, *J. Comput. Chem.* 1996, **17**, 1571.
18) R. Raucoules, T. de Bruin, P. Raybaud and C. Adamo, *Organometallics* 2009, **28**, 5358.
19) S. Tobisch and T. Ziegler, *J. Am. Chem. Soc.* 2004, **126**, 9059.